



Chemical characteristics of cloud water and the impacts on aerosol properties at a subtropical mountain site in Hong Kong

Tao Li^{1,2}, Zhe Wang¹, Yaru Wang¹, Chen Wu^{1,2}, Yiheng Liang¹, Men Xia¹, Chuan Yu¹, Hui Yun¹, Weihao Wang¹, Yan Wang², Jia Guo³, Hartmut Herrmann^{2,4} and Tao Wang¹

5 ¹Department of Civil and Environmental Engineering, The Hong Kong Polytechnic University, Hong Kong, China

²School of Environmental Science and Engineering, Shandong University, Qingdao 266237, China

³Research Center for Eco-Environmental Sciences, Chinese Academy of Sciences, Beijing 100085, China

⁴Leibniz Institute for Tropospheric Research (TROPOS), Permoserstrasse 15, 04318 Leipzig, Germany

Correspondence to: Zhe Wang (z.wang@polyu.edu.hk)

10 **Abstract.** To investigate the cloud water chemistry and the effects of cloud processes on aerosol properties, comprehensive field observations of cloud water, aerosols, and gas-phase species were conducted at a mountaintop site in Hong Kong in October and November 2016. The chemical composition of cloud water including water-soluble ions, dissolved organic matter (DOM), carbonyl compounds, carboxylic acids, and trace metals was quantified. The measured cloud water was very acidic with a mean pH of 3.63, as the ammonium ($174 \mu\text{eq L}^{-1}$) was insufficient for neutralizing the dominant sulfate ($230 \mu\text{eq L}^{-1}$) and nitrate ($160 \mu\text{eq L}^{-1}$). Substantial DOM was found in cloud water, with carbonyl compounds and carboxylic acids accounting for 18.2% and 5.6%, respectively. Different from previous observations, concentrations of methylglyoxal ($19.1 \mu\text{M}$) and glyoxal ($6.72 \mu\text{M}$) were higher than that of formaldehyde ($1.59 \mu\text{M}$). The partitioning of carbonyls between cloud water and the gas phase was also investigated. The measured aqueous fractions of dicarbonyls were comparable to the theoretical estimations, while significant aqueous-phase supersaturation was found for less soluble monocarbonyls, suggesting complicated effects of both physical and chemical processes. In-cloud oxidation played an important role in increasing DOM and sulfate in the cloud water. Abundant glyoxal is suggested to be the most likely precursor of cloud water organics. The aqueous formation of organics was enhanced by photochemistry and under less-acidic conditions. Moreover, as a result of the cloud processes, DOM mass fractions were found to be significantly elevated in in-cloud aerosols, which was likely to contribute to the increase in droplet-mode mass fraction of cloud processed aerosols. This study demonstrates the significant role of clouds in altering the chemical composition and physical properties of aerosols via scavenging and aqueous processes, and provides valuable information about aerosol–cloud interactions in subtropical and coastal regions.

1 Introduction

Ubiquitous clouds in the troposphere play a key role in atmospheric aqueous-phase chemistry by acting as efficient media for the in-cloud formation of sulfate and secondary organic aerosol (SOA) (Harris et al., 2013; Ervens, 2015). Numerous studies on cloud and fog chemistry have been conducted in Europe and North America since the 1990s (Collett et al., 2002; Ervens,



2015; van Pinxteren et al., 2016). During the past decade, studies of the compositions of cloud/fog water, cloud scavenging and aqueous-phase reactions have also been carried out in Asia, particularly in China and Japan (Aikawa et al., 2007; Guo et al., 2012). In-cloud sulfate production, which causes acid rain, has been extensively characterized (Harris et al., 2013; Guo et al., 2012). Recently, more attention has been given to organic materials, which are present in comparable amounts as sulfate and nitrate in cloud and fog water (Collett et al., 2008; Herckes et al., 2013), because of the significant contribution of in-cloud processes to aqueous SOA (aqSOA) formation in high-humidity environments (Ervens et al., 2011; Huang et al., 2011; Tomaz et al., 2018).

Many field observations and laboratory studies have reported direct evidence for the in-cloud formation of low-volatile products and aqSOA. Kaul et al. (2011) observed enhanced SOA production and increased ratios of organic to elemental carbon (OC/EC) upon fog evaporation due to aqueous-phase chemistry. Comparison of the mass spectra of ambient aerosols and cloud organics suggests that functionalization of dissolved organics possibly dominates the formation of SOA through oxidative cloud processes (Lee et al., 2012). A chamber study showed faster SOA formation (by a factor of 2) from isoprene photo-oxidation under cloud conditions than dry conditions (Brégonzio-Rozier et al., 2016), highlighting the importance of aqueous-phase reactions. Aircraft measurements by Sorooshian et al. (2007) found ubiquitous layers of enhanced organic acids levels above clouds, implying that the in-cloud formation of organic acids contributes significantly to emerging organic aerosol layers after droplet evaporation. Oxalate, an aqueous-phase oxidation product, has been considered as a good tracer for aqSOA formation, given the common in-cloud formation pathway of oxalate and sulfate (Yu et al., 2005; Sorooshian et al., 2006). Single-particle mass spectrometry analysis confirmed that oxalate contained in cloud droplet residuals and cloud interstitial particles were three times as abundant as that in cloud-free particles (Zhang et al., 2017), demonstrating the in-cloud formation of oxalate. At present, soluble dicarbonyls are recognized as the primary precursors of carboxylic acids and oligomers in the aqueous phase (Lim et al., 2010; Ervens et al., 2011). The irreversible uptake and aqueous oxidation of glyoxal, the simplest dicarbonyl compound, is suggested to be the primary formation pathway of oxalic acid and aqSOA (Warneck, 2003; Carlton et al., 2007). In general, water-soluble organic compounds (e.g., carbonyls) can partition into cloud droplets and form low-volatility products such as carboxylic acids and oligomers, which stay in the particle phase after cloud evaporation and form aqSOA (Blando and Turpin, 2000; Lim et al., 2005; van Pinxteren et al., 2005; Carlton et al., 2007; Lim et al., 2010; Galloway et al., 2014; Brégonzio-Rozier et al., 2016).

Cloud processes not only contribute to aerosol mass production but also alter the chemical composition of aerosols. Highly oxidized aqSOA usually exhibits higher O/C ratios (1–2) compared to SOA formed in the gas phase (0.3–0.5) (Ervens et al., 2011). Even in the same O/C ratio ranges, the organic compositions of atmospheric particles and cloud water are quite different because of hydrolysis of organosulfate and formation of nitrogen-containing compounds by cloud processing (Boone et al., 2015). In-cloud formation of organics and sulfate is likely to add substantial mass to droplet-mode particles (Ervens et al., 2011). For example, maximum droplet-mode organics and a shift in particle mass size distribution were observed in a simulated cloud process (Brégonzio-Rozier et al., 2016). However, our current knowledge of aqSOA formation mechanisms and how aerosol properties change during real cloud processes remains limited.



The Hong Kong and Pearl River Delta (PRD) region is one of the most industrialized areas in Asia, and experiences serious particulate and photochemical air pollution. High cloudiness and abundant water vapor lead to significant gas–cloud–aerosol interactions in this region, and half of all surface SOA are estimated to be contributed by the aqueous chemistry of dicarbonyls (Li et al., 2013). To better understand the role of cloud processes in aerosol production and the associated changes in its physicochemical properties, we conducted a comprehensive field campaign with simultaneous measurements of trace gases, aerosols and cloud water at a mountaintop site in Hong Kong. In this paper, we first present an analysis of the chemical composition of cloud water and then discuss the partitioning of individual carbonyl compounds between gaseous and aqueous phases. Finally, the effects of cloud processes on cloud water organics formation, aerosol mass production, and aerosol properties are investigated.

10 2 Methodology

2.1 Observation site and sampling

The field campaign was carried out at the summit of Mt. Tai Mo Shan (Mt. TMS, 22°24'N, 114°16'E, 957 m a.s.l.), the highest point of Hong Kong in the southeastern PRD region (Wang et al., 2016), where the coastal and subtropical climate leads to frequent occurrence of cloud/fog events. The site is influenced by both urban/regional pollution from the PRD region and cleaner marine air masses from the western Pacific Ocean. Cloud water, aerosols, and gas-phase carbonyl compounds were simultaneously sampled from 9 October to 22 November 2016.

Cloud water samples were collected in a 500 mL acid-cleaned HPDE bottle by using a single-stage Caltech Active Strand Cloudwater Collector (CASCC) with a flow rate of 24.5 m³ min⁻¹. A detailed description of the collector can be found in our previous work (Guo et al., 2012). The sampling duration was set to 1–3 hours to obtain enough sample volume. Cloudwater pH and electrical conductivity were measured on site using a portable pH meter (model 6350M, JENCO). After filtration through 0.45 μm microfilters (ANPEL Laboratory Technologies (Shanghai) Inc.), aliquots of the cloud water samples for dissolved organic carbon (DOC, 30 ml), carbonyl compounds (20 ml), water-soluble ions (15 ml), organic acids (15 ml, add 5% (v/v) chloroform added) and trace metals (15 ml, 1% (v/v) hydrochloric acid added) were properly prepared and stored at 4 °C in the dark until laboratory analysis. Derivatization of carbonyl compounds with 2,4-dinitrophenylhydrazine (DNPH) was performed on site after adjusting the pH to 3.0 using a buffer solution of citric acid and sodium citrate. Interstitial gas-phase carbonyl compounds were sampled with acidified DNPH-coated silica cartridges (Waters Sep-Pak DNPH-silica) at a flow rate of 0.5 L min⁻¹ for 2–4 hours using a semi-continuous cartridge sampler (ATEC Model 8000). A Teflon filter assembly and an ozone scrubber were installed before the cartridge to remove large droplets and particles and prevent the influence of ozone. All cartridges were refrigerated at -20 °C after sampling.

Daily PM_{2.5} samples were collected on quartz filters (47 mm diameter, Pall Inc.) using a four-channel sampler (Thermo Anderson, RAAS-400, USA) with a flow rate of 16.7 L min⁻¹ and sampling duration of 23 hours. The sample filters were then refrigerated at -20 °C before laboratory analysis. An ambient ion monitor (AIM; URG 9000) was used to measure the hourly



concentrations of water-soluble ions in $PM_{2.5}$. A NanoScan SMPS nanoparticle sizer (Model 3910, TSI Inc.) and an Optical Particle Sizer (OPS) spectrometer (Model 3330, TSI Inc.) were used to measure particle mass size distributions in the range of 0.01 to 9.05 μm with 29 size bins at 1-minute scan intervals. Because of instrument test and failure, the valid data for AIM and particle size distribution were only available from 2 to 11 November and 3 to 21 November, respectively. Trace gases including SO_2 , NO_x , and O_3 were measured with a pulsed UV fluorescence analyzer (Thermo, Model 43c), a chemiluminescence analyzer (Thermo, Model 42i) and a UV photometric analyzer (Thermo, Model 49i), respectively. Hourly $PM_{2.5}$ mass concentration data were provided by the Hong Kong Environmental Protection Department. Ambient temperature and relative humidity were measured using a MetPak Weather Station (Gill, UK), and the solar radiation was monitored using a spectral radiometer (Meteorologie Consult GmbH, Germany).

10 2.2 Laboratory chemical analysis

Water-soluble organic carbon (WSOC) in $PM_{2.5}$ sample filters was extracted with 20 ml Milli-Q water (18.25 $M\Omega$ cm, Millipore) via sonication for 30 min and then filtration. The DOC in cloud water and WSOC in $PM_{2.5}$ were quantified by nondispersive infrared detection of CO_2 after thermocatalytic oxidation at 650 $^{\circ}C$ using a TOC analyzer (Shimadzu TOC-L, Japan). Sucrose standards were used for calibration, with a method detection limit of 0.112 $mg\ L^{-1}$. The dissolved organic matter (DOM) in cloud water (or $PM_{2.5}$ aerosols) was estimated to be 1.8 times of DOC (or WSOC) (van Pinxteren et al., 2016).

The DNPH-derivatives of carbonyl compounds in the cloud water samples were extracted into 20 ml dichloromethane for three times. The extract was then concentrated to dry yellow powder by reduced pressure distillation at 38 $^{\circ}C$ and transferred into 2 ml a high-pressure liquid chromatography (HPLC) grade acetonitrile. The sampled cartridge of gas-phase carbonyl compounds was eluted with 2 ml HPLC grade acetonitrile to a volumetric flask. The cloud water and cartridge extracts were analyzed using HPLC system (PerkinElmer 200 Series) equipped with a UV detector. The method detection limits were determined to be 0.22 μM for formaldehyde, 0.02 μM for acetaldehyde, 0.13 μM for acetone, 0.13 μM for propanal, 0.05 μM for butanal, 0.09 μM for iso-pentanal, 0.06 μM for p-tolualdehyde, 0.07 μM for glyoxal and 0.15 μM for methylglyoxal. The recovery rate ranged from 81% to 98% for individual carbonyls.

Concentrations of water-soluble ions (Na^+ , NH_4^+ , K^+ , Mg^{2+} , Ca^{2+} , Cl^- , NO_3^- and SO_4^{2-}) in the cloud water samples were measured using an ion chromatograph (Dionex, ICS 1000). Four carboxylic acids (acetic, formic, pyruvic and oxalic acids) were analyzed using an ion chromatograph (Dionex, ICS 2500), with an IonPac AS11-HC separator column under NaOH gradient elution. Trace metals including Al, V, Cr, Mn, Fe, Ni, Cu, As, Se, Cd, Ba and Pb were measured by inductively coupled plasma mass spectrometry (ICP-MS, Agilent 7500a) based on the EPA 200.8 method. More details on the ions and trace metal analyses were described in our previous works (Guo et al., 2012; Li et al., 2015).

2.3 Aqueous-phase partitioning fraction of carbonyl compounds

The measured partitioning fraction of carbonyl compounds in the aqueous phase (F_{me}) is calculated by Eq.1,



$$F_{\text{me}} = \frac{C_{\text{cw}}}{C_{\text{cw}} + C_{\text{int}}} \quad (1)$$

where C_{cw} is the air equivalent concentration of carbonyl compounds in cloud water, $\mu\text{g m}^{-3}$; and C_{int} is the interstitial gas-phase carbonyl compounds concentration, $\mu\text{g m}^{-3}$.

Assuming equilibrium, the theoretical aqueous-phase partitioning fraction (F_{theo}) can be calculated from the following equation
5 (van Pinxteren et al., 2005),

$$F_{\text{theo}} = \frac{K_H R T \text{LWC} \cdot 10^{-6}}{1 + K_H R T \text{LWC} \cdot 10^{-6}} \quad (2)$$

where K_H is the Henry's law constant, M atm^{-1} ; R is the gas constant of $0.08205 \text{ L atm mol}^{-1} \text{ K}^{-1}$; T is the mean temperature in K ; and LWC is the cloud liquid water content, g m^{-3} .

3 Results and discussion

10 3.1 Characterization of cloud water chemistry

Thirty-two cloud water samples in six cloud events were collected at Mt. TMS in Hong Kong during the campaign (Figure S1). The averaged LWC was 0.26 g m^{-3} with a range of $0.08\text{--}0.53 \text{ g m}^{-3}$. Cloud water pH ranged between 2.96 and 5.94 with a volume-weighted mean (VWM) value of 3.63, lower than the cloud and fog pH observed in most other areas (e.g., Mt. Tai: 3.86 (Guo et al., 2012); Baengnyeong Island: 3.94 (Boris et al., 2016); Lulin mountain, Taiwan: 3.91 (Simon, 2016);
15 southeastern Pacific: 4.3 (Benedict et al., 2012); and Mt. Schmücke, Germany: 4.30 (van Pinxteren et al., 2016)), indicating the severe acidification of cloud water in this region.

3.1.1 Overview of chemical composition of cloud water

Table 1 summarizes the VWM concentrations of water-soluble ions, DOC, carboxylic acids, carbonyl compounds and trace metals in the cloud water samples. The concentrations of sulfate, nitrate and ammonium ions were 230.8, 160.1 and $173.8 \mu\text{eq L}^{-1}$, respectively, accounting for 80.8% of the total measured ions. The sulfate and nitrate concentrations were much lower
20 L^{-1} , respectively, accounting for 80.8% of the total measured ions. The sulfate and nitrate concentrations were much lower than those in clouds in northern China (Guo et al., 2012) and in fogs at Baengnyeong Island (Boris et al., 2016), but higher than those in many sites in America, Europe and Taiwan (Straub et al., 2012; van Pinxteren et al., 2016; Simon, 2016). Meanwhile, there was insufficient ammonium to neutralize the acid ions, as indicated by the low slope (0.46) of charge balance between $[\text{NH}_4^+]$ and $[\text{NO}_3^- + \text{SO}_4^{2-}]$. The elevated Cl^- ($108.9 \mu\text{eq L}^{-1}$) and Na^+ ($68.7 \mu\text{eq L}^{-1}$) indicated the considerable influence
25 of maritime air from the western Pacific Ocean. In contrast to the commonly observed chloride depletion in coastal cloud water (Benedict et al., 2012), the molar ratio of Cl^-/Na^+ (1.86) at Mt. TMS was obviously higher than the sea-salt ratio (1.16). The abundant Cl^- in cloud water can be ascribed to potential anthropogenic chloride sources (e.g., coal-fired power plants, biomass burning) in the PRD region (Wang et al., 2016). Non-sea-salt sulfate (nss-SO_4^{2-}) was determined to be $96.4 \pm 2.6\%$ of total sulfate based on the $\text{SO}_4^{2-}/\text{Na}^+$ molar ratio in seawater (0.06), demonstrating that SO_4^{2-} was mainly derived from in-cloud
30 oxidation of SO_2 (Harris et al., 2013; Guo et al., 2012) rather than marine source.



Table 1. Concentrations of inorganic and organic species in cloud water samples measured at Mt. TMS during November 2016.

	Unit	VWM	Average	Min	Max
pH	-	3.63	3.87	2.96	5.94
Na ⁺	μeq L ⁻¹	68.7	93.0	3.8	447.0
NH ₄ ⁺	μeq L ⁻¹	173.8	234.9	0.9	1412.7
K ⁺	μeq L ⁻¹	4.1	7.5	BDL	53.6
Mg ²⁺	μeq L ⁻¹	15.3	22.7	BDL	104.9
Ca ²⁺	μeq L ⁻¹	13.9	49.1	BDL	660.8
Cl ⁻	μeq L ⁻¹	108.9	138.5	0.3	616.9
NO ₃ ⁻	μeq L ⁻¹	160.1	237.6	3.9	1284.9
SO ₄ ²⁻	μeq L ⁻¹	230.8	305.3	3.0	1339.5
DOC	mgC L ⁻¹	9.3	12.9	2.0	108.6
Formic	μM	10.8	17.1	0.2	201.8
Acetic	μM	7.2	10.2	0.6	88.2
Pyruvic	μM	1.5	2.7	0.2	22.7
Oxalic	μM	8.3	10.3	7.6	17.5
Formaldehyde	μM	1.59	2.10	BDL	6.35
Acetaldehyde	μM	0.03	0.04	BDL	0.11
Acetone	μM	0.76	0.77	BDL	2.42
Propanal	μM	0.26	0.34	BDL	1.42
Butanal	μM	0.08	0.09	BDL	0.19
iso-pentanal	μM	5.90	7.05	0.63	22.9
p-tolualdehyde	μM	0.36	0.39	BDL	1.16
Glyoxal	μM	6.72	9.00	0.73	47.9
Methylglyoxal	μM	19.1	26.7	BDL	45.0
Al	μg L ⁻¹	131.9	180.2	23.2	737.8
V	μg L ⁻¹	7.9	9.5	0.2	35.7
Cr	μg L ⁻¹	0.7	1.2	BDL	5.0
Mn	μg L ⁻¹	5.9	10.9	0.9	42.6
Fe	μg L ⁻¹	50.6	106.5	BDL	316.8
Ni	μg L ⁻¹	7.1	7.7	0.2	33.0
Cu	μg L ⁻¹	10.0	17.3	BDL	85.9
As	μg L ⁻¹	6.7	7.4	0.7	22.2
Se	μg L ⁻¹	1.9	2.6	0.1	11.5
Cd	μg L ⁻¹	0.5	0.8	BDL	2.9
Ba	μg L ⁻¹	3.0	7.2	BDL	25.1
Pb	μg L ⁻¹	18.7	23.2	0.2	117.9

BDL: below detection limit



DOC concentrations varied from 2.0 to 108.6 mgC L⁻¹ with a VWM value of 9.3 mgC L⁻¹, lower than those in polluted urban fogs but much higher than most remote and marine clouds (Herckes et al., 2013; van Pinxteren et al., 2016; Ervens et al., 2013; Benedict et al., 2012). The VWM concentrations of formic, acetic, pyruvic and oxalic acids were measured to be 10.8, 7.2, 1.5 and 8.3 μM, respectively, accounting for 5.6 ± 2.2% (molar ratio of carbon) of the DOC in total. The formic-to-acetic acid (F/A) ratio in the air has been used to estimate the sources of carboxylic acids in rainwater and cloud water, assuming that they reach gas-liquid equilibrium (Fornaro and Gutz, 2003; Servant et al., 1991; Wang et al., 2011b). Lower (<1) or higher (>1) F/A ratios indicate direct emissions or secondary formation of carboxylic acids, respectively (Wang et al., 2011b). In this study, a remarkable correlation between formic and acetic acid ($r = 0.97$, $p < 0.01$) suggests their similar sources or formation pathways, while the mean F/A ratio of 1.18 (varying from 0.41 to 1.89 in different cloud events, Table S1) indicates the more importance of secondary formation for cloud water carboxylic acids.

Carbonyl compounds (Table 1) comprised 18.2 ± 10.4% of DOC in cloud water. Methylglyoxal (19.1 μM) was the predominated carbonyl species, followed by glyoxal (6.72 μM), iso-pentanal (5.90 μM) and glycolaldehyde (3.56 μM), while formaldehyde (1.59 μM) and acetaldehyde (0.03 μM) were much lower. The greater abundance of cloud water methylglyoxal compared to glyoxal and formaldehyde at Mt. TMS differed from many other observations, for example, at Whistler, Canada (Ervens et al., 2013), Puy de Dôme, France (Deguillaume et al., 2014) and Mt. Schmücke, Germany (van Pinxteren et al., 2005), where glyoxal was more abundant than methylglyoxal but much less than formaldehyde. These differences could, at least partially, be attributable to the higher level of toluene (2208 ppt) than xylene (319 ppt) and isoprene (41 ppt) measured at Mt. TMS (Lam et al., 2013), as different precursors could lead to different yields of glyoxal and methylglyoxal (Ervens et al., 2011).

Aluminium (131.9 μg L⁻¹) dominated the cloud water trace metals, of which the concentration was comparable to that measured at other mountain sites in China (Li et al., 2017). Abundant transition metals Fe (50.6 μg L⁻¹), Cu (10.0 μg L⁻¹) and Mn (5.9 μg L⁻¹), which played important roles in the heterogeneous catalytical formation of sulfate (Harris et al., 2013), were also found. The toxic Pb concentration in cloud water (18.7 μg L⁻¹) was tens of times higher than that in Europe (Fomba et al., 2015) and America (Straub et al., 2012), probably due to traffic emissions from the surrounding city-cluster. Relatively high concentrations of V (7.9 μg L⁻¹) and Ni (7.1 μg L⁻¹) implied notable impacts of residual oil combustion from shipping emissions (Viana et al., 2009; Wang et al., 2014). Clearly, the cloud water at Mt. TMS was significantly influenced by anthropogenic emissions.

3.1.2 Comparisons among different air masses

Three-days backward trajectories were reconstructed using the HYbrid Single-Particle Lagrangian Integrated Trajectory (HYSPLIT) model to investigate the origins of air masses arriving at Mt. TMS, which were influenced by both continental and marine air masses. Three types of air mass plumes for the six cloud events (E.1–6) are identified and displayed in Figure 1: continental (E.1–2), mixed (E.3–4) and marine (E.5–6). Detailed descriptions are given in Table S1.

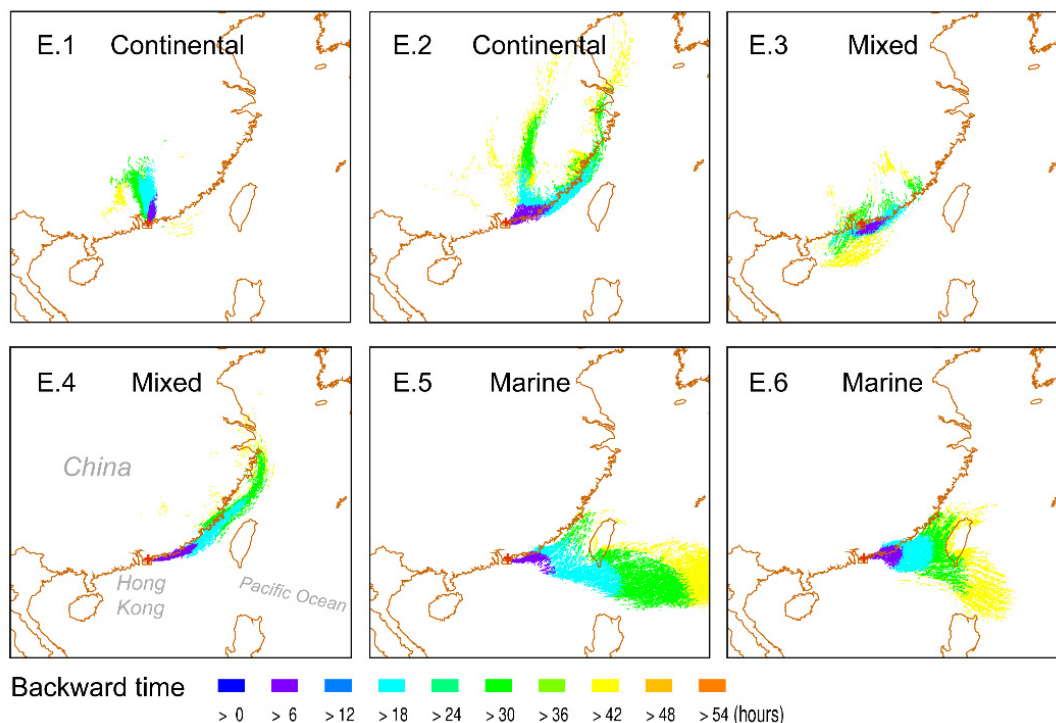


Figure 1. Air mass plumes arriving at Mt. TMS (red plus sign) in Hong Kong for six cloud events (E.1–6) simulated using the HYbrid Single-Particle Lagrangian Integrated Trajectory (HYSPLIT) model.

The concentration distributions of major components of cloud water during six cloud events are compared in Figure 2a. In general, continental air masses brought more abundant major components including DOM, SO_4^{2-} , NO_3^- and Ca^{2+} compared with marine ones, which had lower total concentrations but higher proportions of Cl^- and Na^+ . For example, polluted continental E.1 exhibited the largest amount of major components (393.9 mg L^{-1}) whereas marine E.6 had the least (15.7 mg L^{-1}). For each event, DOM dominated the major components (29–53%), followed by SO_4^{2-} (17–28%) and NO_3^- (17–30%). $\text{Nss-SO}_4^{2-}/\text{NO}_3^-$ ratios in E.1 (1.03) and E.3 (0.91) were lower than in other events (1.38–1.69), indicating the strong influence of regional air masses from the PRD region. The elevated NO_x from traffic emissions in the HK-PRD region (Zheng et al., 2009) is likely to be responsible for the higher nitrate proportions and lower $\text{nss-SO}_4^{2-}/\text{NO}_3^-$ ratios in these two events. Ca^{2+} mainly existed in continental cloud water and the 3% of Ca^{2+} in E.1 likely contributed to the higher pH (5.50). Influenced by marine air masses, the proportions of Cl^- and Na^+ notably increased from 0.4% and 2% in continental cloud water to 5% and 11% in the marine one, respectively. Meanwhile, the equivalent molar ratios of Cl^-/Na^+ and $\text{Ca}^{2+}/\text{Na}^+$ decreased from 3.11 and 5.06 to 1.50 and 0.04, respectively, close to their ratios in seawater (Table S1). Figure 2a shows elevated proportions of V were observed in marine-influenced E.4–6, which is consistent with plumes passing over the busy international shipping routes (Figure S2), suggesting the contribution of residual oil combustion by shipping to coastal cloud water chemistry (Gao et al., 2016).

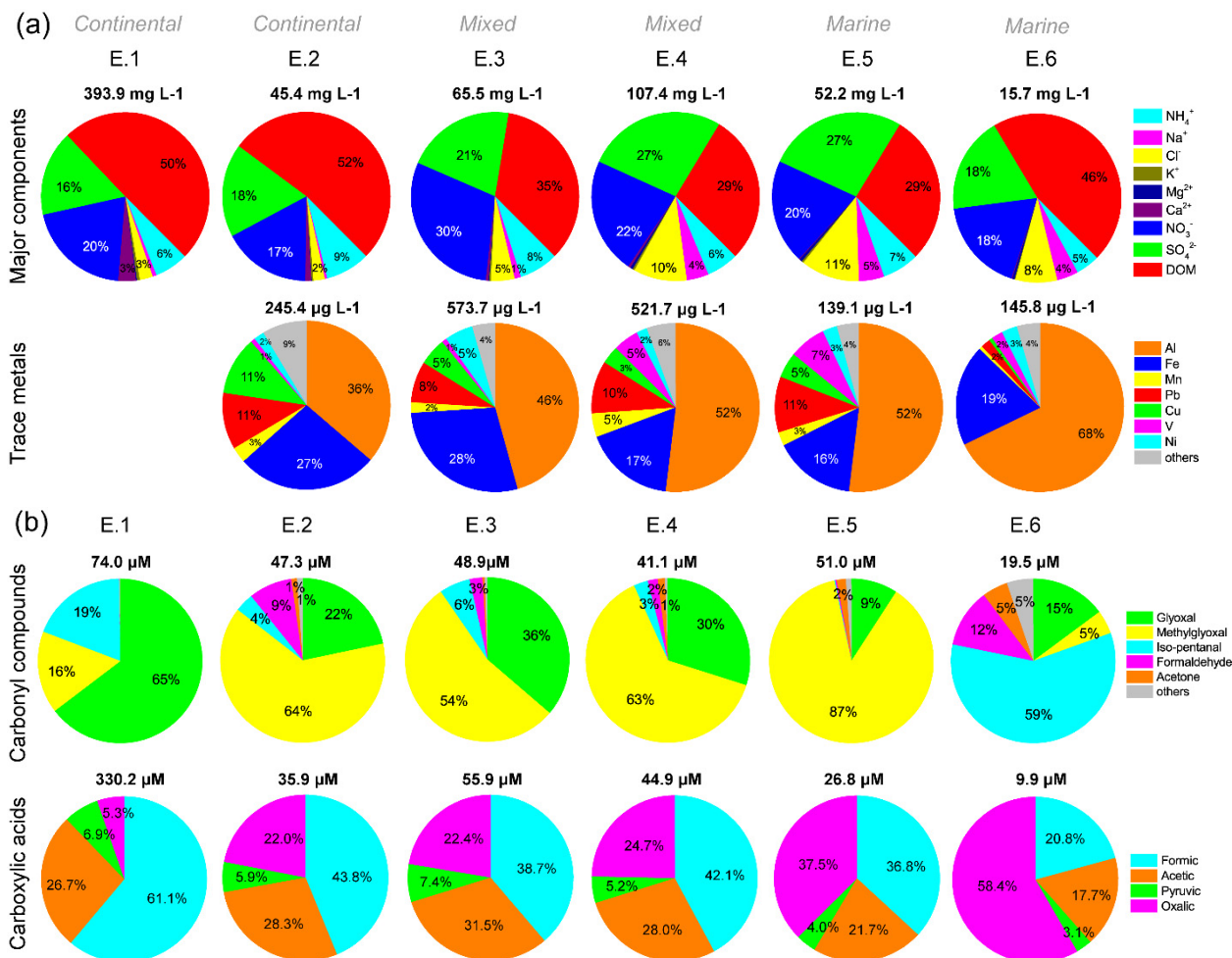


Figure 2. Concentration distributions of (a) major components and trace metals, and (b) carbonyl compounds and carboxylic acids in cloud water for each cloud event (E.1–6). The volume-weighted mean concentrations of individual species are used. Percentages of carbonyl compounds and carboxylic acids in DOC are determined by carbon molar concentration. Trace metals are absent from E.1 due to limited sample volume.

Similar trends for the carbonyl compounds and carboxylic acids with major components can also be seen in Figure 2b, but the distribution patterns are obviously distinct. Methylglyoxal dominated the carbonyl compounds in E.2–5, accounting for 54–87% of total carbonyls. In contrast, glyoxal (65%) became the major species in E.1, followed by iso-pentanal (19%) and methylglyoxal (16%); meanwhile, iso-pentanal (59%) was dominant in E.6, which had more glyoxal (15%) than methylglyoxal (5%). The concentration ratios of formaldehyde/acetaldehyde (C1/C2) and acetaldehyde/propanal (C2/C3) in the gas phase during E.3–6 were calculated (Table S2), to diagnose the possible sources of carbonyls in cloud events. The C1/C2 ratios in the range of 2.83–4.53 suggest the combined contributions of both anthropogenic emissions and biogenic sources to the measured carbonyls, because C1/C2 ratios are normally 1 to 2 for urban areas but close to 10 for the rural forests, due to more photochemical production of formaldehyde than acetaldehyde from natural hydrocarbons (Servant et al., 1991; Possanzini et



al., 1996; Ho et al., 2002). As propanal is believed to be associated only with anthropogenic emissions, the C2/C3 ratio, which is high in rural atmosphere and low in polluted urban air, can be used as an indicator of anthropogenic origin of carbonyl compounds (Possanzini et al., 1996). The average C2/C3 ratios recorded for Mt. TMS were 4.71 ± 2.67 , similar to those measured in roadside and urban environments in Hong Kong (5.0 ± 0.8) (Cheng et al., 2014), indicating the significant anthropogenic sources (e.g., vehicle emissions) of carbonyls at Mt. TMS.

The proportions of oxalic acid notably increased from 5.3 % to 58.4% under the influence of marine air masses, although the total concentrations decreased. High F/A ratios in E.2–5 (1.18–1.89) demonstrated the more importance of secondary formation of carboxylic acids (i.e., aqueous oxidation). However, F/A ratios in E.1 and E.6 were calculated to be 0.41 and 0.50, respectively, indicating the dominant influence of primary emissions in these two events. The concentration and proportion of iso-pentanal in E.1 (14.02 μM , 19%) and E.6 (11.37 μM , 59%) were notably higher than that in other events, possibly resulting from direct sources, although this is unconfirmed.

3.1.3 Relationship of cloud water composition with LWC and pH

LWC and pH are important factors influencing solute concentrations in cloud water. Figure 3 and Figure S3 show the relationships of individual chemical species with LWC and pH. The non- and semi-volatile species in cloud water at Mt. TMS including water-soluble ions, DOC, carboxylic acids and trace metals were inversely related to LWC in the power functions due to dilution effects, which have been widely observed in previous studies (Herckes et al., 2013; Li et al., 2017). Similar inverse-power relationships of water-soluble ions, DOC and carboxylic acids with pH were also found. Increased air pollution and secondary acid ions formation likely made the cloud water more acidic, in turn promoting the dissolution of trace metals (Li et al., 2017). However, carbonyl compounds behaved unexpectedly nonmonotonic relationships with LWC and pH. For example, glyoxal drastically decreased in power function as LWC and pH increased, whereas methylglyoxal exhibited a linearly increasing tendency. The increase and decrease in other carbonyls concentrations with increased LWC and pH are shown in Figure S3. In addition to aqueous-phase reactions, the aqueous/gas phase partitioning of each carbonyl compounds influenced by LWC and pH is another possible reason for the observed relationships (Lim et al., 2010; Ervens et al., 2013; Ervens et al., 2011).

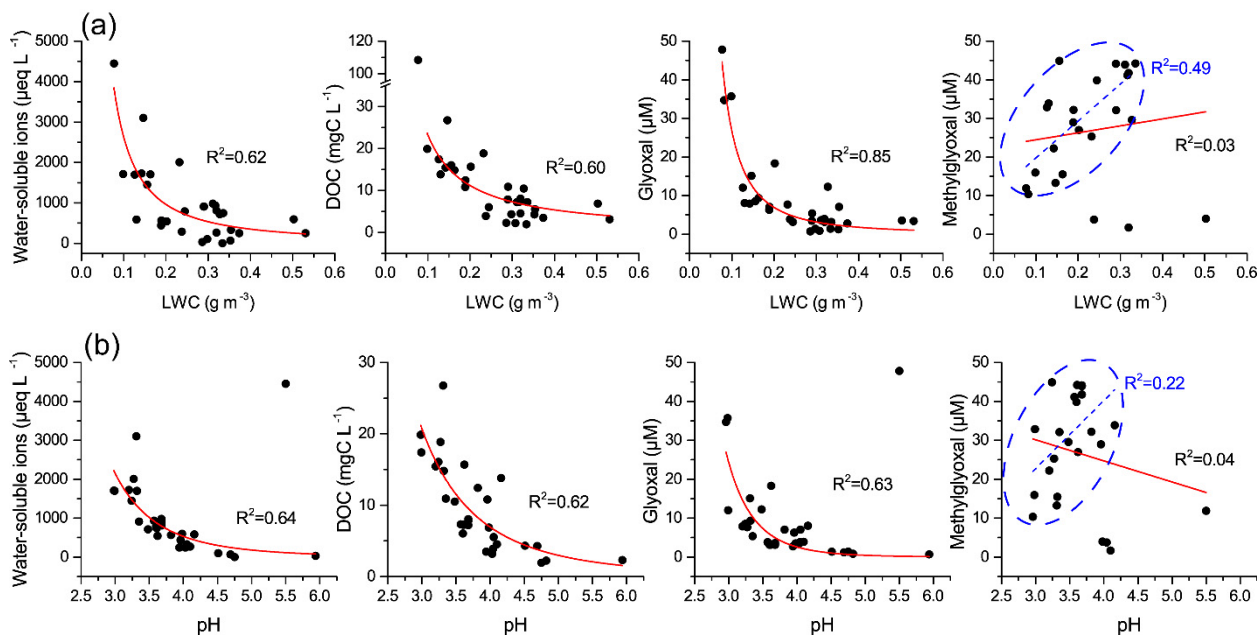


Figure 3. Relationships of water-soluble ions, dissolved organic carbon (DOC), glyoxal and methylglyoxal with (a) liquid water content (LWC) and (b) pH. Methylglyoxal has better linear fitting curves for samples within blue dotted circles.

5 3.2 Aqueous-phase partitioning of carbonyl compounds

The simultaneous measurement of carbonyl compounds in both gas and aqueous phases enables the investigation of their partitioning between different phases (Figure 4 (a) and Table S3). Acetone, formaldehyde, and acetaldehyde were the dominant species (92.6%) measured in the gas phase during cloud events, while methylglyoxal (3.6%) and glyoxal (1.0%) were the minors. Due to high K_H (and solubility) (Table S3), the dicarbonyls were found much more abundant in cloud water, with methylglyoxal and glyoxal accounting for 62.8% and 28.9% of total species, respectively, despite their low gas-phase mixing ratios. However, diverse discrepancies were observed between the measured (F_{me}) and theoretical (F_{theo}) aqueous-phase partitioning fractions of the individual carbonyl compounds. The F_{me}/F_{theo} ratios for each carbonyl are plotted as a function of K_H in Figure 4b. The F_{me} values for carbonyls with small K_H were about 1–3 orders of magnitude higher than F_{theo} , while for highly soluble dicarbonyls the F_{me}/F_{theo} ratios approached unity, similar to the result found at Schmücke mountain in the FEBUKO study (van Pinxteren et al., 2005). Oligomerization on droplets surface layer induced by chemical production and adsorption may lead to the supersaturation of less-soluble carbonyls in cloud water, but it cannot sufficiently explain the supersaturation alone (van Pinxteren et al., 2005; Li et al., 2008).

The “salting” effect is of particular importance in the effective uptake of carbonyl compounds such as glyoxal and methylglyoxal by concentrated solutions (e.g., sulfate, nitrate) (Waxman et al., 2015). Recently, Shen et al. (2018) found that partitioning of six carbonyls to particles was enhanced by more than two orders of magnitude compared to the Henry’s law prediction, which was partially explained by the observed “salting-in” effect (i.e., an increased solubility of organics with salt concentration), a result inconsistent with the laboratory “salting-out” effect (Waxman et al., 2015), due to the more complex



composition of ambient atmosphere and particles. However, the cloud water sulfate molality (~ 0.1 mol kg^{-1} LWC on average) is far from high enough to cause significant “salting” effect, and the effective Henry’s law partitioning of carbonyls in the dilute cloud water at Mt. TMS would only be affected very slightly. It is noteworthy that the K_H employed for less soluble carbonyls refers to pure water as solvent, which may be underestimated in ambient cloud water as influenced by various factors (e.g., hydration and heterogeneous reactions). Considering the hydration reactions, the effective Henry’s law constants for glyoxal (4.2×10^5 M atm^{-1}) (Ip et al., 2009) and methylglyoxal (3.2×10^4 M atm^{-1}) (Zhou and Mopper, 1990) were used to calculate their equilibrium partitioning fractions in the aqueous phase, which consequently agreed with F_{theo} . Formaldehyde was deficient in the cloud water, with a $F_{\text{me}}/F_{\text{theo}}$ value of 0.12, similar to the result reported by Li et al. (2008). This deficiency was probably associated with aqueous oxidation of formaldehyde (Li et al., 2008) and hydroxymethanesulfonate formation with S(IV) (Rao and Collett, 1995; Shen et al., 2012), although the detailed mechanism is uncertain here.

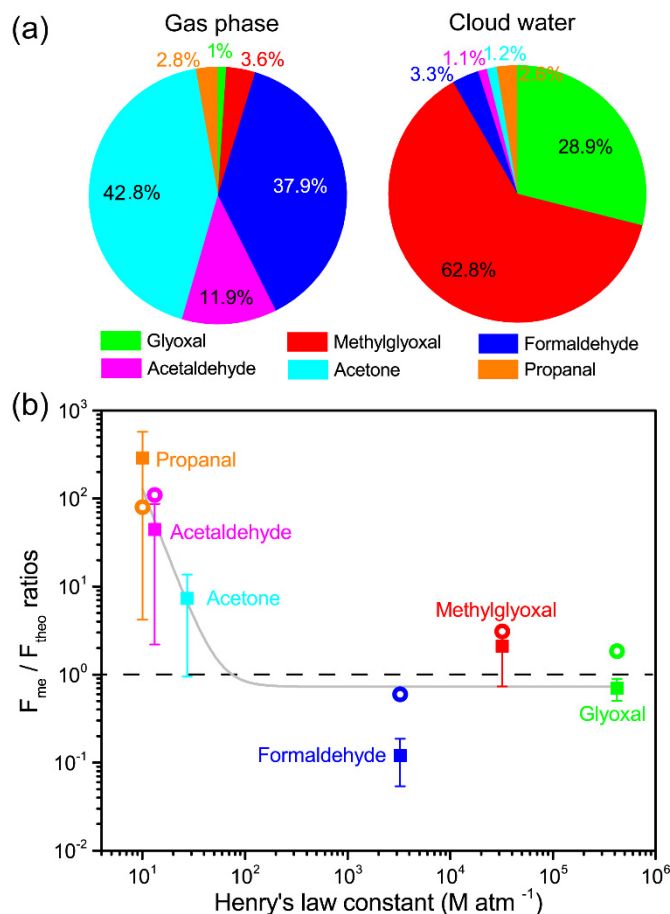
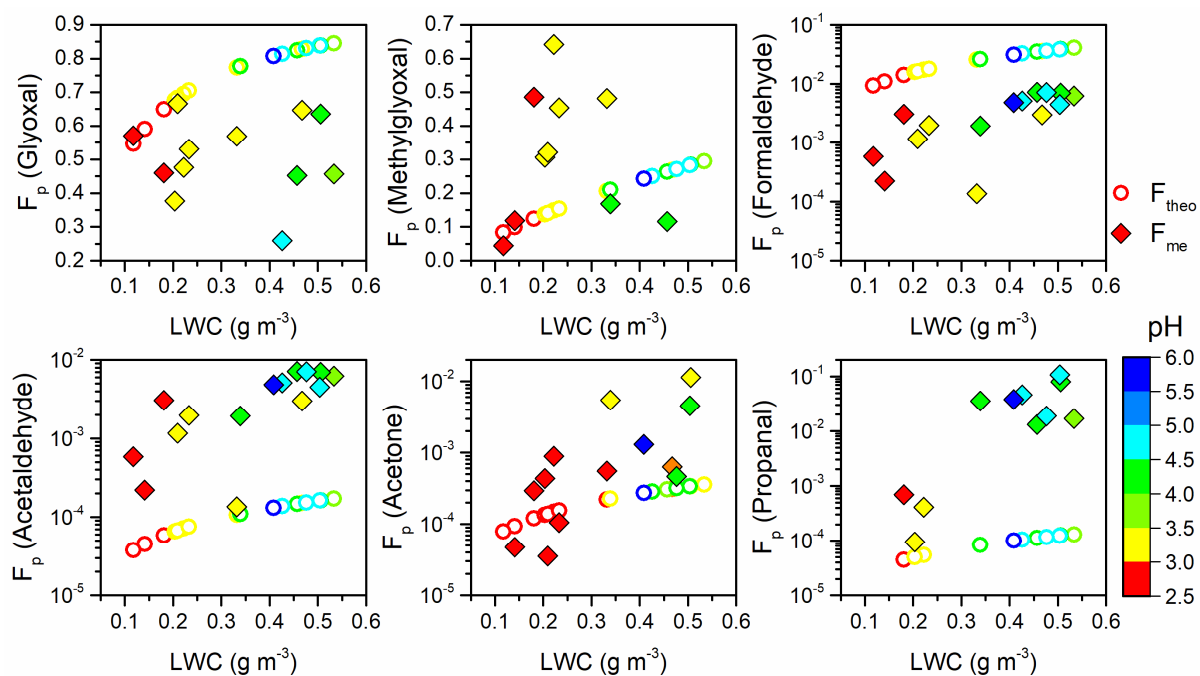


Figure 4. (a) Mass concentration fractions of measured carbonyl compounds in gas phase and cloud water, and (b) $F_{\text{me}}/F_{\text{theo}}$ ratios as a function of Henry’s law constant (K_H). Colored squares represent the mean $F_{\text{me}}/F_{\text{theo}}$ ratios and whiskers indicate standard deviation. For comparison, $F_{\text{me}}/F_{\text{theo}}$ ratios measured at Schmücke mountain (van Pinxteren et al., 2005) are indicated by open circles. The gray fitted line shows the decreasing trend of $F_{\text{me}}/F_{\text{theo}}$ ratios with increasing Henry’s law constant for all species. The dashed line indicates the $F_{\text{me}}/F_{\text{theo}}$ ratio of 1.

15



Figure 5 depicts the dependence of F_{me}/F_{theo} ratios of carbonyl compounds on LWC and pH. In general, the F_{theo} of measured carbonyls increased to different degrees with enhanced LWC, because larger water content has a greater capacity to retain organic species. The F_{me} also increased remarkably as the LWC increased, but deviated to different degrees from F_{theo} . For example, the F_{me} values for methylglyoxal and acetone surpassed their F_{theo} values when LWC exceeded $\sim 0.2 \text{ g m}^{-3}$, whereas the F_{me} values of formaldehyde and acetaldehyde were approximately parallel to their F_{theo} throughout the LWC range, being one order of magnitude lower and higher, respectively. Cloud water acidity may contribute to the deviation between F_{me} and F_{theo} for individual carbonyl compounds. It should be noted that pH value was positively related to LWC but not involved in the F_{theo} calculation, so the elevated F_{theo} and increase in pH were not necessarily correlated. In contrast, the F_{me} seemed to be more close to F_{theo} at lower pH, but increased more rapidly than F_{theo} at higher pH for the monocarbonyls except formaldehyde. For dicarbonyls, the F_{me} of glyoxal slightly decreased at higher pH and showed a larger departure from F_{theo} , while the F_{me} of methylglyoxal far exceeded the theoretical values around pH of 3.0–3.5. The above complicated partitioning behaviours could be affected by both physical (e.g., interface adsorption effect) and chemical processes (e.g., reactions producing less-soluble organics and/or consuming dicarbonyls) (van Pinxteren et al., 2005, and references therein). It is not currently possible to account for the results in detail. Further laboratory and theoretical studies are critically warranted.

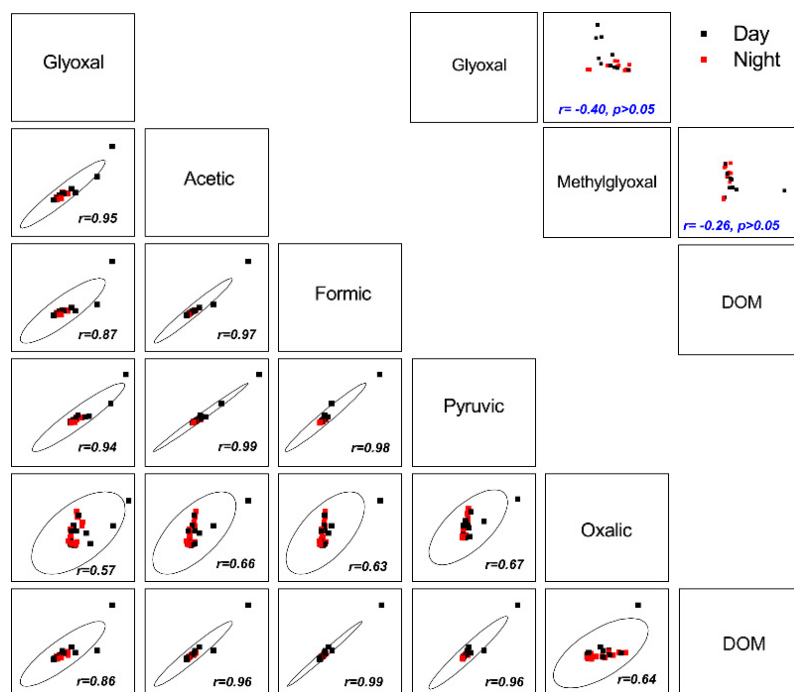


15

Figure 5. Theoretical (F_{theo} , open circle) and measured (F_{me} , solid diamond) aqueous-phase fraction (F_p) of carbonyl compounds as a function of liquid water content (LWC) and pH.

3.3 Correlations between carbonyls and carboxylic acids

To investigate the potential precursors of carboxylic acids and DOM in cloud water, the correlations among all detected organic compounds and water-soluble ions were examined. Significant correlations were found for secondary water-soluble ions (SO_4^{2-} , NO_3^- and NH_4^+) with glyoxal ($r=0.76\text{--}0.88$, $p<0.01$) and carboxylic acids ($r=0.72\text{--}0.94$, $p<0.01$). As sulfate is primarily produced by in-cloud S(IV) oxidation (Harris et al., 2013), a strong correlation ($r=0.75$, $p<0.01$) between oxalic acid and sulfate suggests significant in-cloud formation of oxalic acid. Likewise, the cloud process might have contributed to the secondary formation of other organic matters in the aqueous phase, such as DOM with a significant correlation with sulfate ($r = 0.83$, $p < 0.01$) (Ervens et al., 2011; Yu et al., 2005).



10 **Figure 6. Pairwise scatter plot of selected organic species in cloud water. The ellipses indicate confidence coefficient of 99%.**

Figure 6 shows the pairwise correlations ($p<0.01$) among selected organic species. Aqueous-phase glyoxal was positively correlated with all carboxylic acids ($r = 0.57\text{--}0.95$) and DOM ($r = 0.86$) in both daytime and nighttime. Moreover, the gas-phase glyoxal performed positive relationships with aqueous-phase glyoxal and carboxylic acids, particularly oxalic acid (Figure S4). Many laboratory experiments (Lim et al., 2010; Lee et al., 2011; Schaefer et al., 2015; Sui et al., 2017) have demonstrated that radical (mainly $\cdot\text{OH}$) and non-radical aqueous oxidation of glyoxal can produce abundant small carboxylic acids (e.g., oxalic and formic acids), oligomers and highly oxidized organics, which subsequently lead to mass increase in SOA upon droplet evaporation (Galloway et al., 2014; Gomez et al., 2015). In this study, the abundant methylglyoxal showed no significant correlations with glyoxal, carboxylic acids or DOM in both daytime and nighttime. Therefore, given the high solubility of glyoxal and its potential yield of carboxylic acids (Carlton et al., 2007; Lim et al., 2005; Lim et al., 2010; Blando



and Turpin, 2000), glyoxal is likely to be the most important precursor of secondary organic matters in cloud water at Mt. TMS. Thus, the consumption of glyoxal in the oxidation reactions may partially contribute to its slight unsaturation in the aqueous phase (Figure 5). In addition, as oxalic acid is predominantly formed in clouds (Myriokefalitakis et al., 2011; Ervens et al., 2011), the good interrelationships among carboxylic acids and DOM (Figure 6) indicates that carboxylic acids can directly contribute to DOM formation and/or contribute indirectly by oxidizing to oligomers (Carlton et al., 2006; Tan et al., 2012).

3.4 Aqueous organics formation and cloud effects on aerosol properties

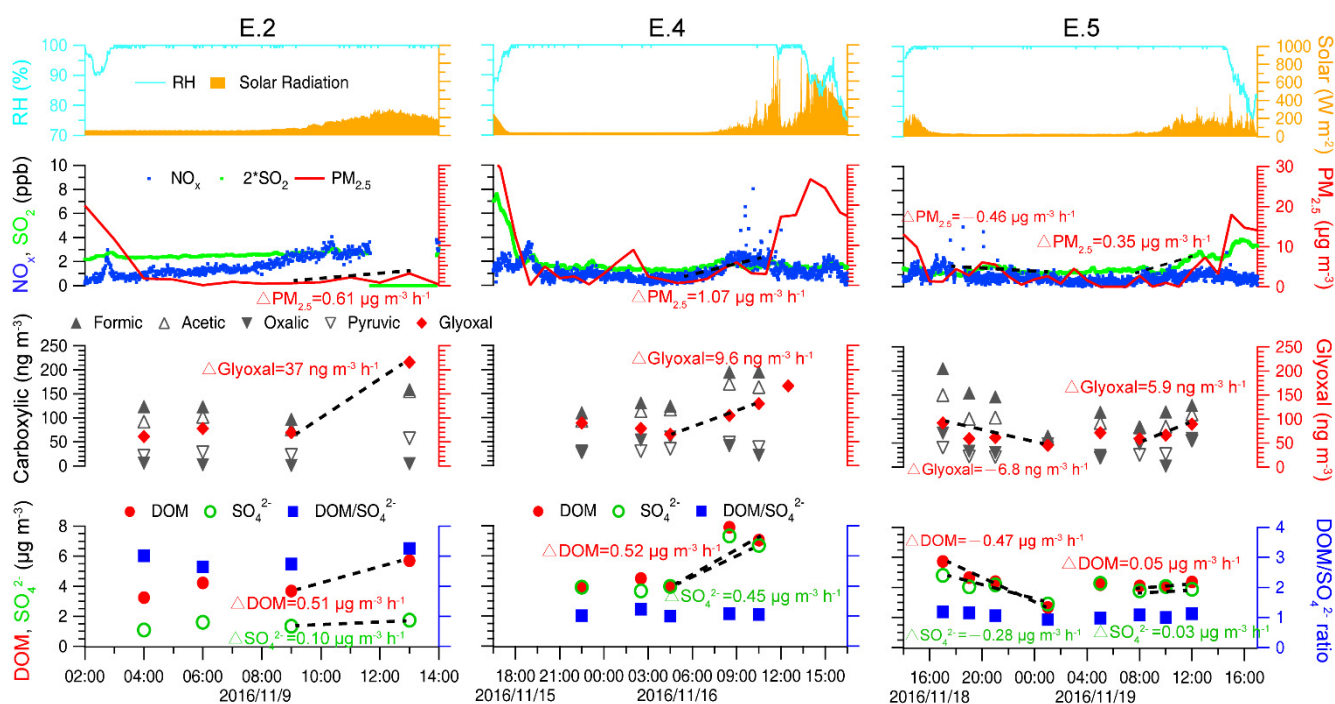
3.4.1 Variation of cloud water organics and aerosol particles

Cloud processes can efficiently remove aerosol particles from the air by nucleation scavenging and impaction scavenging (Ervens, 2015), especially at the initial stage of cloud events (Wang et al., 2011a; Li et al., 2017). At the same time, cloud processes greatly favor the in-cloud formation of sulfate (Harris et al., 2013) and SOA (Brégonzio-Rozier et al., 2016). To investigate the scavenging and changes of aerosols during cloud events, temporal variations of glyoxal, carboxylic acids, DOM and sulfate in cloud water, and ambient $PM_{2.5}$ during three cloud events (E.2, E.4, and E.5) were examined (Figure 7). Based on hourly $PM_{2.5}$ and water-soluble ions data (not shown here), the averaged scavenging ratios were determined to be 0.72 for $PM_{2.5}$, 0.85 for aerosol sulfate, 0.69 for nitrate and 0.68 for ammonium within the first 1–2 h of cloud processes, which were ascribed to the high cloud density, long cloud duration and little external aerosol invasion.

Figure 7 illustrates the variations of cloud water organics, sulfate and ambient $PM_{2.5}$ along with cloud evolution. Positive change rates were found during the daytime with enhanced solar radiation, while negative change rates appeared with reduced solar radiation at sunset and nighttime. This result agreed with the simulation by Huang et al. (2011), in which increasing solar radiation enhanced organic acids and SOA production through photolysis reactions. During the clean continental case E.2, carboxylic acids in cloud water increased by 2–5 times and DOM was elevated from 3.7 to 5.7 $\mu\text{g m}^{-3}$ as solar radiation intensified to $\sim 300 \text{ W m}^{-2}$, corresponding to the dramatic growth in aqueous glyoxal from 69 to 216 ng m^{-3} ; while the increment of sulfate was relatively small, with only 0.15 $\mu\text{g m}^{-3}$ (i.e., 10%). The ratios of oxalic/sulfate and DOM/sulfate increased from 0.6×10^{-3} to 2.6×10^{-3} and from 2.7 to 3.3, respectively, similar to the aircraft observation of increased oxalate/sulfate ratio in aerosols above clouds (Sorooshian et al., 2007), which indicated much more efficient in-cloud formation of oxalate and DOM relative to sulfate. A chamber study demonstrated that the faster photochemical uptake of glyoxal under irradiation than that in dark conditions remarkably enhanced the aqSOA formation rate by several orders of magnitude (Volkamer et al., 2009), and the radical-initiated photo-production of aqSOA mass in the daytime was predicted to be an order of magnitude higher than at nighttime (Ervens and Volkamer, 2010). Therefore, the increase in daytime $PM_{2.5}$ ($0.61 \mu\text{g m}^{-3} \text{ h}^{-1}$) observed during E.2 could be attributed to the cloud water organic matters which have a much higher formation rate than sulfate. During the mixed E.4, the growth rates of DOM ($0.52 \mu\text{g m}^{-3} \text{ h}^{-1}$) and sulfate ($0.45 \mu\text{g m}^{-3} \text{ h}^{-1}$) were comparably fast to induce a high $PM_{2.5}$ growth rate ($1.07 \mu\text{g m}^{-3} \text{ h}^{-1}$). In comparison, the slow growth of DOM ($0.05 \mu\text{g m}^{-3} \text{ h}^{-1}$) and sulfate ($0.03 \mu\text{g m}^{-3} \text{ h}^{-1}$) during



the marine E.5 induced only $0.35 \mu\text{g m}^{-3} \text{h}^{-1}$ of $\text{PM}_{2.5}$. This suggests that the in-cloud formation of both DOM and sulfate influences the fine aerosol production. It was also noted that aqueous glyoxal gradually increased after sunrise, which likely produced carboxylic acids such as oxalic acid rapidly via photo-oxidation of glyoxal and contributed to formation of aqueous organics (Carlton et al., 2007; Warneck, 2003). Although aqueous-phase oligomers can be formed at nighttime, their contributions to aqSOA formation are too small to compensate for the organic losses compared to aqueous photo-oxidation reactions during the daytime (Ervens et al., 2011). In E.5, the decrease in nighttime glyoxal ($-6.8 \text{ ng m}^{-3} \text{h}^{-1}$) was accompanied by the reduction of carboxylic acids and loss of DOM ($-0.47 \mu\text{g m}^{-3} \text{h}^{-1}$), which could be responsible for the net decrease in $\text{PM}_{2.5}$ mass ($-0.46 \mu\text{g m}^{-3} \text{h}^{-1}$).



10 **Figure 7. Temporal variation of air equivalent concentrations of glyoxal, carboxylic acids, dissolved organic matter (DOM), SO_4^{2-} and $\text{DOM}/\text{SO}_4^{2-}$ ratio in cloud water, and ambient $\text{PM}_{2.5}$ during three cloud events (E.2, E.4 and E.5). Meteorological parameters (relative humidity and solar radiation) and trace gases (NO_x and SO_2) are also displayed. Mass change rates of cloud water components and ambient $\text{PM}_{2.5}$ are indicated by dashed lines and slopes.**

Figure 7 also shows that $\text{DOM}/\text{SO}_4^{2-}$ ratios during E.4 and E.5 remained constant at around 1.0 with stronger cloud water acidity ($\text{pH} = 2.96\text{--}3.68$), whereas the ratios during other cloud events varied from 1.6 to 6.5 under higher pH conditions (3.62–5.94). Figure 8 shows the $\text{DOM}/\text{SO}_4^{2-}$ ratio as a function of pH values and the significantly positive relationship between DOM and sulfate. The $\text{DOM}/\text{SO}_4^{2-}$ ratios reduced under more acidic conditions (lower pH values due to increased sulfate). As the predominant pathway of in-cloud sulfate oxidation by H_2O_2 in the pH range of 3–6 is independent of pH (Seinfeld and Pandis, 2006; Shen et al., 2012), the reduced $\text{DOM}/\text{SO}_4^{2-}$ ratios with lowered pH suggest that DOM production slowed, probably due



to adverse effects of cloud water acidity. Competition for H_2O_2 between carbonyl compounds and S(IV) is unlikely because substantial H_2O_2 is usually found in cloud water (Shen et al., 2012). Sorooshian et al. (2007) found that the production of oxalic acid was more efficient relative to sulfate in larger size and less acidic droplets. Laboratory studies (Gomez et al., 2015; Zhao et al., 2006) also found that the uptake of both glyoxal and methylglyoxal by acidic solutions increased with decreasing acid concentration, contributing to the formation of organic aerosols more efficiently. The observed increase in $\text{DOM}/\text{SO}_4^{2-}$ ratio at higher pH suggests that the in-cloud formation of DOM was much more efficient than sulfate under less acidic conditions.

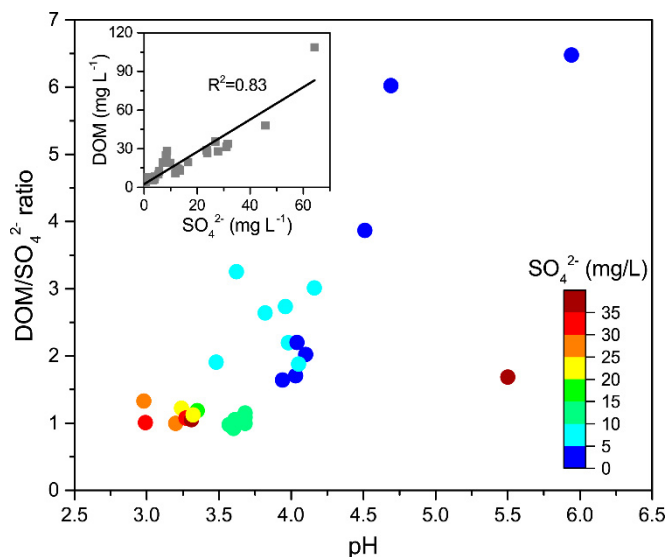


Figure 8. $\text{DOM}/\text{SO}_4^{2-}$ ratio as a function of cloudwater pH value. Color scale represents SO_4^{2-} concentrations in cloud water. The embedded graph shows the relationship between DOM and SO_4^{2-} .

10 3.4.2 Impacts of cloud processes on particle composition and size distribution

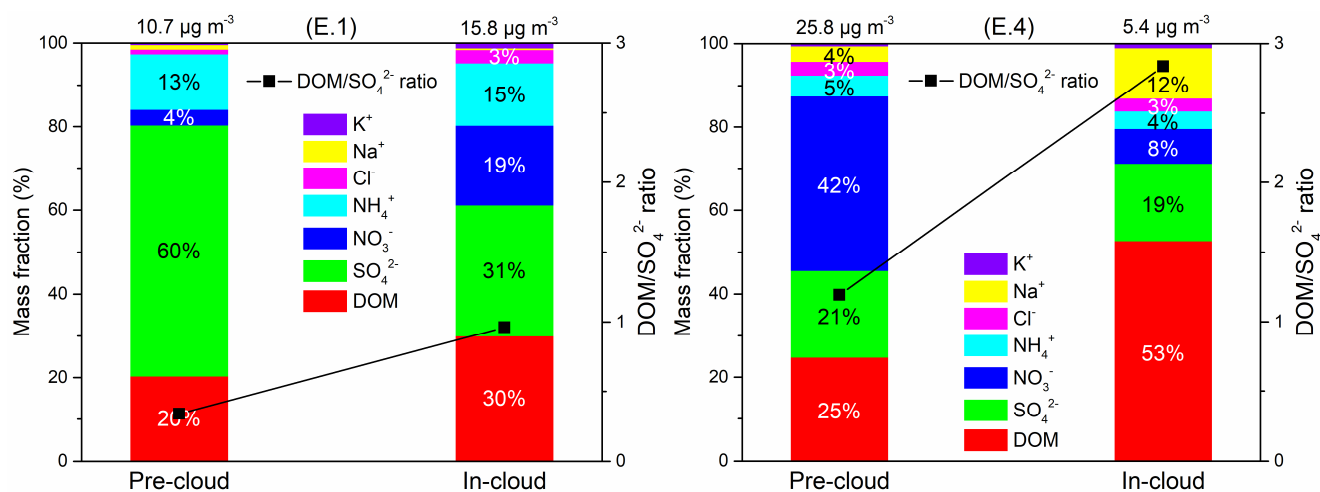
To evaluate the impacts of cloud processes on aerosol chemistry, the major water-soluble components in pre-cloud and in-cloud aerosols ($\text{PM}_{2.5}$) are compared in Figure 9. Except for the highly polluted E.1 case, in which major components were increased in the in-cloud aerosols ($15.8 \mu\text{g m}^{-3}$) compared with the pre-cloud aerosols ($10.7 \mu\text{g m}^{-3}$), the other cloud events showed significant decreases in major components concentrations because of cloud scavenging. The chemical compositions of in-cloud aerosols obviously differed from the pre-cloud aerosols. In the polluted case E.1, sulfate was the most abundant species in pre-cloud aerosols, accounting for 60% of mass concentration, but decreased to 31% in the in-cloud aerosols. Meanwhile, the mass fraction of DOM was elevated from 20% (pre-cloud) to 30% (in-cloud), and nitrate increased from 4% to 19%, probably due to the large increase in NO_2 (over 4-fold). For the mixed case E.4, DOM mass fraction in the in-cloud aerosols was twice that of pre-cloud aerosols, consistent with the increasing trend of DOM in cloud water shown in Figure 7.

15

20 It has been suggested that highly oxidized cloud water organics readily remain in evaporating cloud droplets and contribute to aqSOA mass production, whereas semi-volatile products are prone to escape into the gas phase (Schurman et al., 2018). However, the $\text{DOM}/\text{SO}_4^{2-}$ ratios for in-cloud aerosols during both cloud events were about 3 times greater than that for pre-



cloud aerosols, although the ratios did not change much in corresponding cloud water, implying that the oxidized cloud water organics are predominantly retained in aerosols. Overall, the evidently increased DOM mass fraction and DOM/SO₄²⁻ ratios in the in-cloud aerosols indicated the significance of cloud processes in the aqSOA formation.

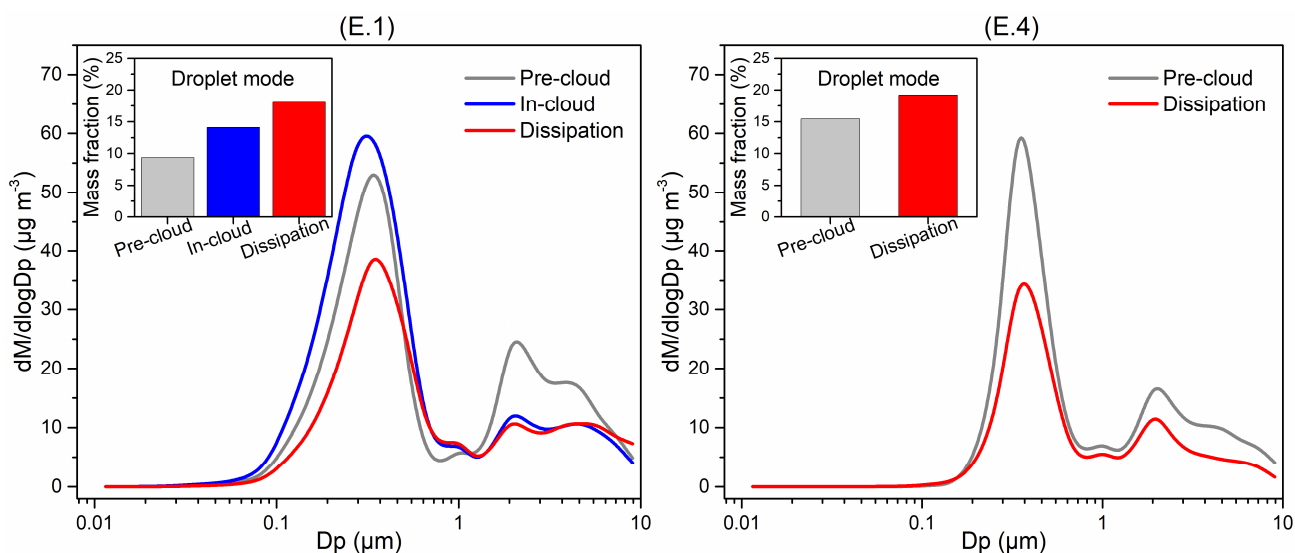


5 **Figure 9. Mass concentration distributions of major water-soluble components and DOM/SO₄²⁻ ratios in the pre-cloud and in-cloud PM_{2.5} during cloud events E.1 (left) and E.4 (right).**

In Figure 10, the averaged mass size distributions of aerosols during different cloud periods are compared. Multimodal distribution is apparent, with the dominant accumulation mode peaking at ~0.4 μm and a second coarse mode at ~2.0 μm. Accumulation-mode aerosols (0.1–1.0 μm) usually consist of two subgroups, the condensation and droplet modes peaking typically at 0.2–0.3 and 0.5–0.8 μm, respectively (Hinds, 2012). In this study, the overlapping of the two subgroups likely made the accumulation mode peak and a small peak near 1.0 μm. During the polluted E.1, the accumulation-mode aerosols exhibited higher concentrations than the pre-cloud aerosols, whereas the coarse aerosols were largely scavenged. As cloud dissipated, accumulation-mode aerosols decreased, while the concentrations of aerosols with a diameter of over 0.6 μm remained the same as the in-cloud ones. The droplet-mode (0.5–1.0 μm) mass fraction increased significantly after the cloud process, growing from the pre-cloud 9.3% to 14.1% (in-cloud) and 18.0% (dissipation periods). For the mixed event E.4, the cloud-processed particles also showed an elevated droplet-mode mass fraction (19.2%) compared to the pre-cloud particles (15.2%), even though particles were scavenged in all modes. As droplet-mode particles are mainly produced from aqueous reactions, the increase in droplet-mode mass fraction after cloud dissipation may be associated with the in-cloud formation of sulfate and aqSOA (Blando and Turpin, 2000; Ervens et al., 2011). We propose that the substantial DOM (air equivalent concentration of 15.0 μg m⁻³) and sulfate (4.9 μg m⁻³) measured in cloud water are mostly retained in droplet-mode particles upon cloud evaporation. This proposition is supported by the abundant droplet-mode oxalate, organic carbon and sulfate aerosols reported in Hong Kong (Bian et al., 2014; Gao et al., 2016), although the mass size distributions of particle compositions were not measured in this study. In addition, given the elevated DOM fractions and DOM/SO₄²⁻ mass ratios in



the in-cloud aerosols (Figure 9), aqSOA formation seemed to play a more important role than sulfate in producing droplet-mode particles.



5 **Figure 10.** Averaged mass size distributions of aerosols during the pre-cloud, in-cloud and dissipation periods for cloud events E.1 and E.4. Embedded graphs show the droplet-mode particles fraction of the total mass.

4 Conclusions

Gas–cloud–aerosol interactions can change the fate of trace gases and the physicochemical properties of aerosols, but the multiphase processes in the subtropical PRD–HK region are still poorly understood. This study presents the results from a field campaign with concurrent measurements of gases, particles and cloud waters conducted at a mountain site in Hong Kong for the first time. The chemical compositions of the acidic cloud water (pH=2.96–5.94) during different cloud events were dominated by DOM and secondary inorganic ions, which were heavily influenced by anthropogenic emissions from continental air masses. Continental air masses generally contributed more pollutants to cloud water than the marine air masses did. The distinct relationships of carbonyl compounds with LWC and pH were likely controlled by their partitioning between cloud water and the gas phase. Simultaneous measurements in the two phases enabled the investigation of their partitioning behaviors. The F_{me} values of dicarbonyls considering hydration reactions agreed well with their theoretical values, whereas large discrepancies were found between F_{me} and F_{theo} of monocarbonyls. The complicated partitioning behaviors of carbonyls possibly result from the combined effects of physical adsorption and chemical production/loss, which require further study. The good correlation between DOM and sulfate indicated the in-cloud formation of aqueous organics, for which abundant glyoxal was identified as the most likely precursor. Apart from cloud scavenging of aerosol particles, cloud processes played crucial roles in changing the chemical composition and mass size distribution of particles. During cloud processes, increases in daytime $PM_{2.5}$ ($0.35\text{--}1.07\ \mu\text{g m}^{-3}\ \text{h}^{-1}$) were observed as solar radiation increased, with simultaneously increased glyoxal ($5.9\text{--}37\ \text{ng m}^{-3}\ \text{h}^{-1}$) and net-production of cloud water DOM ($0.05\text{--}0.52\ \mu\text{g m}^{-3}\ \text{h}^{-1}$) and sulfate ($0.03\text{--}0.45\ \mu\text{g m}^{-3}\ \text{h}^{-1}$). The



cloud water DOM production, which is more efficient under less acidic conditions, is likely to have contributed to aerosol mass growth more significantly than sulfate, as the DOM mass fractions in the cloud-processed aerosols were remarkably increased. Moreover, sulfate and DOM produced in cloud water are expected to remain in the particle phase and cause mass increase in droplet-mode particles after cloud dissipation. The observations provide direct evidence for the aqueous formation of secondary aerosols in cloud processes, and promote our understanding of the gas–cloud–aerosol interactions and multiphase chemistry of polluted coastal environments.

Author contribution

ZW, TW and YW designed the research; TL, YW, CW, YL performed the field measurement of cloud water and sample analysis; MX, CY, HY, WW conducted the measurement of trace gases and aerosols; TL, ZW and JG performed data analysis and wrote the manuscript. All authors contributed to discussion and commented on the paper.

Acknowledgments

The authors would like to thank Steven Poon, Bobo Wong for their support during the campaign, and to thank Hong Kong Environmental Protection Department (HKEPD) for sharing the trace gas and PM_{2.5} data at Tai Mo Shan AQM station. This work was funded by the National Key R&D Program of China (2016YFC0200503), Research Grant Council of the Hong Kong Special Administrative Region, China (25221215, 15265516, T24-504/17-N), and the National Natural Science Foundation of China (41605093, 41475115, 41505103). The authors also acknowledge the support of the Research Institute for Sustainable Urban Development (RISUD).

References

- Aikawa, M., Hiraki, T., Suzuki, M., Tamaki, M., and Kasahara, M.: Separate chemical characterizations of fog water, aerosol, and gas before, during, and after fog events near an industrialized area in Japan, *Atmospheric Environment*, 41, 1950-1959, 10.1016/j.atmosenv.2006.10.049, 2007.
- Benedict, K. B., Lee, T., and Collett, J. L.: Cloud water composition over the southeastern Pacific Ocean during the VOCALS regional experiment, *Atmospheric Environment*, 46, 104-114, 10.1016/j.atmosenv.2011.10.029, 2012.
- Bian, Q., Huang, X. H. H., and Yu, J. Z.: One-year observations of size distribution characteristics of major aerosol constituents at a coastal receptor site in Hong Kong - Part 1: Inorganic ions and oxalate, *Atmospheric Chemistry and Physics*, 14, 9013-9027, 10.5194/acp-14-9013-2014, 2014.
- Blando, J. D., and Turpin, B. J.: Secondary organic aerosol formation in cloud and fog droplets: a literature evaluation of plausibility, *Atmospheric Environment*, 34, 1623-1632, [https://doi.org/10.1016/S1352-2310\(99\)00392-1](https://doi.org/10.1016/S1352-2310(99)00392-1), 2000.
- Boone, E. J., Laskin, A., Laskin, J., Wirth, C., Shepson, P. B., Stirm, B. H., and Pratt, K. A.: Aqueous Processing of Atmospheric Organic Particles in Cloud Water Collected via Aircraft Sampling, *Environmental Science & Technology*, 49, 8523-8530, 10.1021/acs.est.5b01639, 2015.



- Boris, A. J., Lee, T., Park, T., Choi, J., Seo, S. J., and Collett Jr, J. L.: Fog composition at Baengnyeong Island in the eastern Yellow Sea: detecting markers of aqueous atmospheric oxidations, *Atmospheric Chemistry and Physics*, 16, 437-453, 10.5194/acp-16-437-2016, 2016.
- 5 Brégonzio-Rozier, L., Giorio, C., Siekmann, F., Pangui, E., Morales, S. B., Temime-Roussel, B., Gratien, A., Michoud, V., Cazaunau, M., DeWitt, H. L., Tapparo, A., Monod, A., and Doussin, J. F.: Secondary organic aerosol formation from isoprene photooxidation during cloud condensation–evaporation cycles, *Atmospheric Chemistry and Physics*, 16, 1747-1760, 10.5194/acp-16-1747-2016, 2016.
- 10 Carlton, A. G., Turpin, B. J., Lim, H.-J., Altieri, K. E., and Seitzinger, S.: Link between isoprene and secondary organic aerosol (SOA): Pyruvic acid oxidation yields low volatility organic acids in clouds, *Geophysical Research Letters*, 33, 10.1029/2005gl025374, 2006.
- Carlton, A. G., Turpin, B. J., Altieri, K. E., Seitzinger, S., Reff, A., Lim, H.-J., and Ervens, B.: Atmospheric oxalic acid and SOA production from glyoxal: Results of aqueous photooxidation experiments, *Atmospheric Environment*, 41, 7588-7602, 10.1016/j.atmosenv.2007.05.035, 2007.
- 15 Cheng, Y., Lee, S. C., Huang, Y., Ho, K. F., Ho, S. S. H., Yau, P. S., Louie, P. K. K., and Zhang, R. J.: Diurnal and seasonal trends of carbonyl compounds in roadside, urban, and suburban environment of Hong Kong, *Atmospheric Environment*, 89, 43-51, 10.1016/j.atmosenv.2014.02.014, 2014.
- Collett, J. L., Bridgman, H. A., and Bendix, J.: Preface, *Atmospheric Research*, 64, 1-2, [https://doi.org/10.1016/S0169-8095\(02\)00074-1](https://doi.org/10.1016/S0169-8095(02)00074-1), 2002.
- 20 Collett, J. L., Herckes, P., Youngster, S., and Lee, T.: Processing of atmospheric organic matter by California radiation fogs, *Atmospheric Research*, 87, 232-241, 10.1016/j.atmosres.2007.11.005, 2008.
- Deguillaume, L., Charbouillot, T., Joly, M., Vaïtilingom, M., Parazols, M., Marinoni, A., Amato, P., Delort, A. M., Vinatier, V., Flossmann, A., Chaumerliac, N., Pichon, J. M., Houdier, S., Laj, P., Sellegri, K., Colomb, A., Brigante, M., and Mailhot, G.: Classification of clouds sampled at the puy de Dôme (France) based on 10 yr of monitoring of their physicochemical properties, *Atmospheric Chemistry and Physics*, 14, 1485-1506, 10.5194/acp-14-1485-2014, 2014.
- 25 Ervens, B., and Volkamer, R.: Glyoxal processing by aerosol multiphase chemistry: towards a kinetic modeling framework of secondary organic aerosol formation in aqueous particles, *Atmospheric Chemistry and Physics*, 10, 8219-8244, 10.5194/acp-10-8219-2010, 2010.
- Ervens, B., Turpin, B. J., and Weber, R. J.: Secondary organic aerosol formation in cloud droplets and aqueous particles (aqSOA): a review of laboratory, field and model studies, *Atmospheric Chemistry and Physics*, 11, 11069-11102, 10.5194/acp-11-11069-2011, 2011.
- 30 Ervens, B., Wang, Y., Eagar, J., Leaitch, W. R., Macdonald, A. M., Valsaraj, K. T., and Herckes, P.: Dissolved organic carbon (DOC) and select aldehydes in cloud and fog water: the role of the aqueous phase in impacting trace gas budgets, *Atmospheric Chemistry and Physics*, 13, 5117-5135, 10.5194/acp-13-5117-2013, 2013.
- Ervens, B.: Modeling the processing of aerosol and trace gases in clouds and fogs, *Chemical reviews*, 115, 4157-4198, 10.1021/cr5005887, 2015.
- 35 Fomba, K. W., van Pinxteren, D., Müller, K., Iinuma, Y., Lee, T., Collett, J. L., and Herrmann, H.: Trace metal characterization of aerosol particles and cloud water during HCCT 2010, *Atmospheric Chemistry and Physics*, 15, 8751-8765, 10.5194/acp-15-8751-2015, 2015.
- Fornaro, A., and Gutz, I. G. R.: Wet deposition and related atmospheric chemistry in the São Paulo metropolis, Brazil: Part 2—contribution of formic and acetic acids, *Atmospheric Environment*, 37, 117-128, 2003.
- 40 Galloway, M. M., Powelson, M. H., Sedehi, N., Wood, S. E., Millage, K. D., Kononenko, J. A., Rynaski, A. D., and De Haan, D. O.: Secondary organic aerosol formation during evaporation of droplets containing atmospheric aldehydes, amines, and ammonium sulfate, *Environmental Science & Technology*, 48, 14417-14425, 10.1021/es5044479, 2014.
- Gao, Y., Lee, S.-C., Huang, Y., Chow, J. C., and Watson, J. G.: Chemical characterization and source apportionment of size-resolved particles in Hong Kong sub-urban area, *Atmospheric Research*, 170, 112-122, 10.1016/j.atmosres.2015.11.015, 2016.
- 45 Gomez, M. E., Lin, Y., Guo, S., and Zhang, R.: Heterogeneous chemistry of glyoxal on acidic solutions. An oligomerization pathway for secondary organic aerosol formation, *The Journal of Physical Chemistry A*, 119, 4457-4463, 10.1021/jp509916r, 2015.



- Guo, J., Wang, Y., Shen, X., Wang, Z., Lee, T., Wang, X., Li, P., Sun, M., Collett, J. L., Wang, W., and Wang, T.: Characterization of cloud water chemistry at Mount Tai, China: Seasonal variation, anthropogenic impact, and cloud processing, *Atmospheric Environment*, 60, 467-476, 10.1016/j.atmosenv.2012.07.016, 2012.
- 5 Harris, E., Sinha, B., van Pinxteren, D., Tilgner, A., Fomba, K. W., Schneider, J., Roth, A., Gnauk, T., Fahlbusch, B., Mertes, S., Lee, T., Collett, J., Foley, S., Borrmann, S., Hoppe, P., and Herrmann, H.: Enhanced role of transition metal ion catalysis during in-cloud oxidation of SO₂, *Science*, 340, 727-730, 10.1126/science.1230911, 2013.
- Herckes, P., Valsaraj, K. T., and Collett, J. L.: A review of observations of organic matter in fogs and clouds: Origin, processing and fate, *Atmospheric Research*, 132-133, 434-449, 10.1016/j.atmosres.2013.06.005, 2013.
- Hinds, W. C.: *Aerosol technology: properties, behavior, and measurement of airborne particles*, John Wiley & Sons, 2012.
- 10 Ho, K. F., Lee, S. C., Louie, P. K. K., and Zou, S. C.: Seasonal variation of carbonyl compound concentrations in urban area of Hong Kong, *Atmospheric Environment*, 36, 1259-1265, [https://doi.org/10.1016/S1352-2310\(01\)00570-2](https://doi.org/10.1016/S1352-2310(01)00570-2), 2002.
- Huang, X. H. H., Ip, H. S. S., and Yu, J. Z.: Secondary organic aerosol formation from ethylene in the urban atmosphere of Hong Kong: A multiphase chemical modeling study, *Journal of Geophysical Research*, 116, 10.1029/2010jd014121, 2011.
- Ip, H. S. S., Huang, X. H. H., and Yu, J. Z.: Effective Henry's law constants of glyoxal, glyoxylic acid, and glycolic acid, *Geophysical Research Letters*, 36, 10.1029/2008gl036212, 2009.
- 15 Kaul, D. S., Gupta, T., Tripathi, S. N., Tare, V., and Collett, J. L.: Secondary organic aerosol: a comparison between foggy and nonfoggy days, *Environmental Science & Technology*, 45, 7307-7313, 10.1021/es201081d, 2011.
- Lam, S. H. M., Saunders, S. M., Guo, H., Ling, Z. H., Jiang, F., Wang, X. M., and Wang, T. J.: Modelling VOC source impacts on high ozone episode days observed at a mountain summit in Hong Kong under the influence of mountain-valley breezes, *Atmospheric Environment*, 81, 166-176, 10.1016/j.atmosenv.2013.08.060, 2013.
- 20 Lee, A. K. Y., Herckes, P., Leaitch, W. R., Macdonald, A. M., and Abbatt, J. P. D.: Aqueous OH oxidation of ambient organic aerosol and cloud water organics: Formation of highly oxidized products, *Geophysical Research Letters*, 38, L11805, 10.1029/2011gl047439, 2011.
- Lee, A. K. Y., Hayden, K. L., Herckes, P., Leaitch, W. R., Liggió, J., Macdonald, A. M., and Abbatt, J. P. D.: Characterization of aerosol and cloud water at a mountain site during WACS 2010: secondary organic aerosol formation through oxidative cloud processing, *Atmospheric Chemistry and Physics*, 12, 7103-7116, 10.5194/acp-12-7103-2012, 2012.
- 25 Li, N., Fu, T.-M., Cao, J., Lee, S., Huang, X.-F., He, L.-Y., Ho, K.-F., Fu, J. S., and Lam, Y.-F.: Sources of secondary organic aerosols in the Pearl River Delta region in fall: Contributions from the aqueous reactive uptake of dicarbonyls, *Atmospheric Environment*, 76, 200-207, 10.1016/j.atmosenv.2012.12.005, 2013.
- 30 Li, S.-M., Macdonald, A. M., Leithead, A., Leaitch, W. R., Gong, W., Anlauf, K. G., Toom-Saunty, D., Hayden, K., Bottenheim, J., and Wang, D.: Investigation of carbonyls in cloudwater during ICARTT, *Journal of Geophysical Research*, 113, 10.1029/2007jd009364, 2008.
- Li, T., Wang, Y., Li, W. J., Chen, J. M., Wang, T., and Wang, W. X.: Concentrations and solubility of trace elements in fine particles at a mountain site, southern China: regional sources and cloud processing, *Atmos. Chem. Phys.*, 15, 8987-9002, 10.5194/acp-15-8987-2015, 2015.
- 35 Li, T., Wang, Y., Zhou, J., Wang, T., Ding, A., Nie, W., Xue, L., Wang, X., and Wang, W.: Evolution of trace elements in the planetary boundary layer in southern China: Effects of dust storms and aerosol-cloud interactions, *Journal of Geophysical Research: Atmospheres*, 10.1002/2016jd025541, 2017.
- Lim, H. J., Carlton, A. G., and Turpin, B. J.: Isoprene forms secondary organic aerosol through cloud processing: model simulations, *Environmental Science & Technology*, 39, 4441-4446, 2005.
- 40 Lim, Y. B., Tan, Y., Perri, M. J., Seitzinger, S. P., and Turpin, B. J.: Aqueous chemistry and its role in secondary organic aerosol (SOA) formation, *Atmospheric Chemistry and Physics*, 10, 10521-10539, 10.5194/acp-10-10521-2010, 2010.
- Myriokefalitakis, S., Tsigaridis, K., Mihalopoulos, N., Sciare, J., Nenes, A., Kawamura, K., Segers, A., and Kanakidou, M.: In-cloud oxalate formation in the global troposphere: a 3-D modeling study, *Atmospheric Chemistry and Physics*, 11, 5761-5782, 10.5194/acp-11-5761-2011, 2011.
- 45 Possanzini, M., Di Palo, V., Petricca, M., Fratarcangeli, R., and Brocco, D.: Measurements of lower carbonyls in Rome ambient air, *Atmospheric Environment*, 30, 3757-3764, [https://doi.org/10.1016/1352-2310\(96\)00110-0](https://doi.org/10.1016/1352-2310(96)00110-0), 1996.
- Rao, X., and Collett, J. L.: Behavior of S(IV) and Formaldehyde in a Chemically Heterogeneous Cloud, *Environmental Science & Technology*, 29, 1023-1031, 1995.



- Schaefer, T., van Pinxteren, D., and Herrmann, H.: Multiphase chemistry of glyoxal: revised kinetics of the alkyl radical reaction with molecular oxygen and the reaction of glyoxal with OH, NO₃, and SO₄⁻ in aqueous solution, *Environmental Science & Technology*, 49, 343-350, 10.1021/es505860s, 2015.
- Schurman, M. I., Boris, A., Desyaterik, Y., and Collett, J. J. L.: Aqueous Secondary Organic Aerosol Formation in Ambient Cloud Water Photo-Oxidations, *Aerosol and Air Quality Research*, 18, 15-25, 10.4209/aaqr.2017.01.0029, 2018.
- Seinfeld, J. H., and Pandis, S. N.: *ATMOSPHERIC CHEMISTRY AND PHYSICS (SECOND EDITION)*[M], JOHN WILEY & SONS, INC., 470-483 pp., 2006.
- Servant, J., Kouadio, G., Cros, B., and Delmas, R.: Carboxylic monoacids in the air of mayombe forest (Congo): Role of the forest as a source or sink, *Journal of Atmospheric Chemistry*, 12, 367-380, 10.1007/bf00114774, 1991.
- Shen, H., Chen, Z., Li, H., Qian, X., Qin, X., and Shi, W.: Gas-Particle Partitioning of Carbonyl Compounds in the Ambient Atmosphere, *Environmental Science & Technology*, 52, 10997-11006, 10.1021/acs.est.8b01882, 2018.
- Shen, X., Lee, T., Guo, J., Wang, X., Li, P., Xu, P., Wang, Y., Ren, Y., Wang, W., Wang, T., Li, Y., Carn, S. A., and Collett, J. L.: Aqueous phase sulfate production in clouds in eastern China, *Atmospheric Environment*, 62, 502-511, 10.1016/j.atmosenv.2012.07.079, 2012.
- Simon, S.: Chemical Composition of Fog Water at Four Sites in Taiwan, *Aerosol and Air Quality Research*, 16, 618-631, 10.4209/aaqr.2015.03.0154, 2016.
- Sorooshian, A., Varutbangkul, V., Brechtel, F. J., Ervens, B., Feingold, G., Bahreini, R., Murphy, S. M., Holloway, J. S., Atlas, E. L., Buzorius, G., Jonsson, H., Flagan, R. C., and Seinfeld, J. H.: Oxalic acid in clear and cloudy atmospheres: Analysis of data from International Consortium for Atmospheric Research on Transport and Transformation 2004, *Journal of Geophysical Research: Atmospheres*, 111, D23S45, 10.1029/2005jd006880, 2006.
- Sorooshian, A., Lu, M. L., Brechtel, F. J., Jonsson, H., Feingold, G., Flagan, R. C., and Seinfeld, J. H.: On the source of organic acid aerosol layers above clouds, *Environmental Science & Technology*, 41, 4647-4654, 2007.
- Straub, D. J., Hutchings, J. W., and Herckes, P.: Measurements of fog composition at a rural site, *Atmospheric Environment*, 47, 195-205, 10.1016/j.atmosenv.2011.11.014, 2012.
- Sui, X., Zhou, Y., Zhang, F., Chen, J., Zhu, Z., and Yu, X. Y.: Deciphering the aqueous chemistry of glyoxal oxidation with hydrogen peroxide using molecular imaging, *Physical Chemistry Chemical Physics*, 19, 20357-20366, 10.1039/c7cp02071f, 2017.
- Tan, Y., Lim, Y. B., Altieri, K. E., Seitzinger, S. P., and Turpin, B. J.: Mechanisms leading to oligomers and SOA through aqueous photooxidation: insights from OH radical oxidation of acetic acid and methylglyoxal, *Atmospheric Chemistry and Physics*, 12, 801-813, 10.5194/acp-12-801-2012, 2012.
- Tomaz, S., Cui, T., Chen, Y., Sexton, K. G., Roberts, J. M., Warneke, C., Yokelson, R. J., Surratt, J. D., and Turpin, B. J.: Photochemical Cloud Processing of Primary Wildfire Emissions as a Potential Source of Secondary Organic Aerosol, *Environmental Science & Technology*, 52, 11027-11037, 10.1021/acs.est.8b03293, 2018.
- van Pinxteren, D., Plewka, A., Hofmann, D., Müller, K., Kramberger, H., Svrčina, B., Bächmann, K., Jaeschke, W., Mertes, S., Collett, J. L., and Herrmann, H.: Schmücke hill cap cloud and valley stations aerosol characterisation during FEBUKO (II): Organic compounds, *Atmospheric Environment*, 39, 4305-4320, 10.1016/j.atmosenv.2005.02.014, 2005.
- van Pinxteren, D., Fomba, K. W., Mertes, S., Müller, K., Spindler, G., Schneider, J., Lee, T., Collett, J. L., and Herrmann, H.: Cloud water composition during HCCT-2010: Scavenging efficiencies, solute concentrations, and droplet size dependence of inorganic ions and dissolved organic carbon, *Atmospheric Chemistry and Physics*, 16, 3185-3205, 10.5194/acp-16-3185-2016, 2016.
- Viana, M., Amato, F., Alastuey, A., Querol, X., Moreno, T., García Dos Santos, S., Herce, M. D., and Fernández-Patier, R.: Chemical Tracers of Particulate Emissions from Commercial Shipping, *Environmental Science & Technology*, 43, 7472-7477, 10.1021/es901558t, 2009.
- Volkamer, R., Ziemann, P. J., and Molina, M. J.: Secondary organic aerosol formation from acetylene (C₂H₂): seed effect on SOA yields due to organic photochemistry in the aerosol aqueous phase, *Atmospheric Chemistry and Physics*, 9, 1907-1928, 2009.
- Wang, T., Tham, Y. J., Xue, L., Li, Q., Zha, Q., Wang, Z., Poon, S. C. N., Dubé, W. P., Blake, D. R., and Louie, P. K. K.: Observations of nitryl chloride and modeling its source and effect on ozone in the planetary boundary layer of southern China, *Journal of Geophysical Research: Atmospheres*, 121, 2476-2489, 2016.



- Wang, Y., Guo, J., Wang, T., Ding, A., Gao, J., Zhou, Y., Collett, J. L., and Wang, W.: Influence of regional pollution and sandstorms on the chemical composition of cloud/fog at the summit of Mt. Taishan in northern China, *Atmospheric Research*, 99, 434-442, 10.1016/j.atmosres.2010.11.010, 2011a.
- 5 Wang, Y., Sun, M., Li, P., Li, Y., Xue, L., and Wang, W.: Variation of low molecular weight organic acids in precipitation and cloudwater at high elevation in South China, *Atmospheric Environment*, 45, 6518-6525, 10.1016/j.atmosenv.2011.08.064, 2011b.
- Wang, Z., Sorooshian, A., Prabhakar, G., Coggon, M. M., and Jonsson, H. H.: Impact of emissions from shipping, land, and the ocean on stratocumulus cloud water elemental composition during the 2011 E-PEACE field campaign, *Atmospheric Environment*, 89, 570-580, 10.1016/j.atmosenv.2014.01.020, 2014.
- 10 Warneck, P.: In-cloud chemistry opens pathway to the formation of oxalic acid in the marine atmosphere, *Atmospheric Environment*, 37, 2423-2427, 10.1016/s1352-2310(03)00136-5, 2003.
- Waxman, E. M., Elm, J., Kurten, T., Mikkelsen, K. V., Ziemann, P. J., and Volkamer, R.: Glyoxal and Methylglyoxal Setschenow Salting Constants in Sulfate, Nitrate, and Chloride Solutions: Measurements and Gibbs Energies, *Environmental Science & Technology*, 49, 11500-11508, 10.1021/acs.est.5b02782, 2015.
- 15 Yu, J. Z., Huang, X. F., Xu, J., and Hu, M.: When aerosol sulfate goes up, so does oxalate: implication for the formation mechanisms of oxalate, *Environmental Science & Technology*, 39, 128-133, 2005.
- Zhang, G., Lin, Q., Peng, L., Yang, Y., Fu, Y., Bi, X., Li, M., Chen, D., Chen, J., Cai, Z., Wang, X., Peng, P., amp, apos, an, Sheng, G., and Zhou, Z.: Insight into the in-cloud formation of oxalate based on in situ measurement by single particle mass spectrometry, *Atmospheric Chemistry and Physics*, 17, 13891-13901, 10.5194/acp-17-13891-2017, 2017.
- 20 Zhao, J., Levitt, N. P., Zhang, R., and Chen, J.: Heterogeneous reactions of methylglyoxal in acidic media: implications for secondary organic aerosol formation, *Environmental Science & Technology*, 40, 7682-7687, 2006.
- Zheng, J., Zhang, L., Che, W., Zheng, Z., and Yin, S.: A highly resolved temporal and spatial air pollutant emission inventory for the Pearl River Delta region, China and its uncertainty assessment, *Atmospheric Environment*, 43, 5112-5122, 10.1016/j.atmosenv.2009.04.060, 2009.
- 25 Zhou, X., and Mopper, K.: Apparent partition coefficients of 15 carbonyl compounds between air and seawater and between air and freshwater; implications for air-sea exchange, *Environmental Science & Technology*, 24, 1864-1869, 10.1021/es00082a013, 1990.